Seeded free-electron and inverse free-electron laser techniques for radiation amplification and electron microbunching in the terahertz range

C. Sung, S. Ya. Tochitsky, S. Reiche, J. B. Rosenzweig, C. Pellegrini, and C. Joshi
Neptune Laboratory, Departments of Electrical Engineering and Physics, University of California, Los Angeles, California 90095, USA
(Received 26 June 2006; published 22 December 2006)

A comprehensive analysis is presented that describes amplification of a seed THz pulse in a single-pass free-electron laser (FEL) driven by a photoinjector. The dynamics of the radiation pulse and the modulated electron beam are modeled using the time-dependent FEL code, GENESIS 1.3. A 10-ps (FWHM) electron beam with a peak current of 50–100 A allows amplification of a ~1 kW seed pulse in the frequency range 0.5–3 THz up to 10–100 MW power in a relatively compact 2-m long planar undulator. The electron beam driving the FEL is strongly modulated, with some inhomogeneity due to the slippage effect. It is shown that THz microbunching of the electron beam is homogeneous over the entire electron pulse when saturated FEL amplification is utilized at the very entrance of an undulator. This requires seeding of a 30-cm long undulator buncher with a 1–3 MW of pump power with radiation at the resonant frequency. A narrow-band seed pulse in the THz range needed for these experiments can be generated by frequency mixing of CO_2 laser lines in a GaAs nonlinear crystal. Two schemes for producing MW power pulses in seeded FELs are considered in some detail for the beam parameters achievable at the Neptune Laboratory at UCLA: the first uses a waveguide to transport radiation in the 0.5–3 THz range through a 2-m long FEL amplifier and the second employs high-gain third harmonic generation using the FEL process at 3–9 THz.

DOI: 10.1103/PhysRevSTAB.9.120703 PACS numbers: 41.60.Cr, 42.72.Ai, 42.65.Ky

I. INTRODUCTION

Free-electron laser (FEL) interactions can be used to generate high-output power radiation or to longitudinally modulate the electron beam in the THz frequency range. The THz range of the electromagnetic spectrum can be conveniently covered by FELs because the electron beam parameters needed are relatively easily realized using current technology. Two FEL configurations can provide THz pulses: an FEL oscillator and a single-pass amplifier. In the first case, a multipass FEL oscillator is driven by a few microsecond long electron beam. The low peak current in the beam and losses attributed with the cavity optics make the task of obtaining high THz peak power difficult. In the second case, a single-pass FEL amplifier based on self-amplified spontaneous emission of radiation (SASE) is capable of producing MW power THz pulses in a very long (~ 6–10 m) undulator [1]. However, in the latter case, the radiation pulse buildup from spontaneous noise makes synchronization with an external event or a laser pulse on a subpicosecond time scale extremely difficult. A promising alternative to SASE FEL is a seeded single-pass FEL amplifier which can significantly shorten the undulator length, thus opening the possibility of driving FELs with a short, high peak current beam and reach a very high FEL gain. However, in the THz range this technique is not studied yet due to the lack of a suitable radiation seed source.

Production of radiation using a periodically undulating electron beam results in its bunching at the resonant frequency. Such bunched electron beams have been successfully generated in several advanced acceleration schemes in vacuum [2,3]. Microbunching on the scale of 1–9 THz is of particular importance for matched injection of a pre-bunched electron beam into a laser-driven or beam-driven plasma accelerating structure [4]. In these experiments, plasma densities are on the order 10^{16}–10^{18} cm^{-3}, which correspond to plasma wavelengths of 330–33 μm, respectively. To modulate an electron beam in this spectral range, both seeded FEL and inverse free-electron laser (IFEL) techniques can be utilized in principle but to date, neither schemes have been tested experimentally.

Recently at the Neptune Laboratory at UCLA we have launched an experimental program towards development of a THz radiation source that can act as a seed for the single-pass FEL amplifier discussed earlier. We propose to use difference-frequency generation (DFG) of CO_2 laser lines in a nonlinear crystal in order to produce narrow-band ($\Delta\nu/\nu \sim 10^{-5}$), high-power seed pulses tunable in the range of 1–3 THz. We have already demonstrated in a single-shot experiment up to 2 MW of power at 1 THz in a 200 ps pulse [5] and in a high repetition rate experiment 2 kW of power in a 200 ns pulse [6]. These developments have stimulated the present study of seeded THz FEL/IFELs driven by a high-peak current photoinjector.

In this paper we analyze seeded FEL/IFEL techniques from the point of view of production of multimegawatt radiation pulses and microbunching of a nominally 10 MeV electron beam on the THz scale. The time-dependent FEL code GENESIS 1.3 is used for analysis. Two possible THz FEL/IFEL experimental schemes are studied in detail using beam parameters of the Neptune S-band photoinjector [7]. First, a high-gain FEL amplifier,

where a kW seed pulse in the 0.5–3 THz range is amplified in a waveguide to tens of MW, is considered. The second scheme is a high-gain harmonic generation (HGHG) FEL, where a short IFEL modulator seeded by a MW power pulse in the 0.5–3 THz range first bunches the beam and is followed by a second radiator-undulator tuned to the third harmonic of the fundamental frequency. The HGHG technique allows extending the spectral range of high-power radiation to 3–9 THz where the needed seed pulse is not easily generated in nonlinear crystals.

II. SIMULATIONS OF A HIGH-GAIN SEEDED THZ FEL AMPLIFIER

A. FEL undulator optimization

It is known that the power increase in a FEL is directly related to the degree of energy modulation of the electrons as they propagate through the undulator. When electrons wiggle inside the undulator and interact with the collinearly propagating seed radiation, the energy modulation of electrons causes electrons to bunch together with the same periodicity as the radiation wavelength. As a result, wiggling electrons emit radiation coherently and the seed radiation is amplified.

When an electron experiences a full cycle of changing of electric field while wiggling one period in the undulator, the energy modulation is maximized. This so-called resonant condition can be written as

$$\lambda = \frac{\lambda_u}{2\gamma^2}\left(1 + \frac{K^2}{2}\right), \tag{1}$$

where $K = eB_u/mck_u$ is the dimensionless undulator parameter, λ is the radiation wavelength, γ the electron Lorentz factor (energy), λ_u the undulator wavelength, k_u the undulator wave number, and B_u the undulator magnetic field. Note that Eq. (1) corresponds to the free-space FEL case. If the radiation propagates in a waveguide, Eq. (1) can be modified by replacing λ with the effective radiation wavelength (λ_{eff}) derived from the dispersion relation of the guiding structure.

As seen in Eq. (1), for any given undulator, the frequency of radiation can be tuned by changing the energy γ of the electron beam to match the desired resonant wavelengths. A seed source based on DFG in a GaAs crystal can generate radiation in the range of 0.5–3 THz [5,6]. Here we consider driving an FEL amplifier with an electron beam from a rf photoinjector (typical electron beam parameters are shown in Table I) and amplifying the frequencies provided by the seed source. The resonant condition is chosen for the study such that $\gamma \sim 26$ and 15 corresponds to $\lambda = 100$ and 300 μm, respectively.

To design the undulator, the optimization of several parameters (such as λ_u, B_u, and gap between the faces of the magnets) needs to be considered. For a meter long or longer undulator, guiding of the THz beam is necessary to minimize the diffraction losses. A rectangular waveguide is chosen to confine the radiation fields and to preserve the polarization. The waveguide size in turn sets a limit on the minimum gap between the pole pieces of the magnet. We use the TE_{01} mode that can cover the whole amplitude of the wiggling motion of the electron beam. On the other hand, λ_u and B_u are chosen to give reasonable values of K to maximize the FEL interaction along the resonant curve of given γ and λ. In addition, the Halbach criterion given by [8]

$$B_{\max} = 3.33 \exp\left[-\frac{Gap}{\lambda_u}\left(5.47 - 1.8\frac{Gap}{\lambda_u}\right)\right], \tag{2}$$

sets a limit on $B_{\max}$, because of the physical restriction in building strong magnets with small periods and gaps.

After several iterations in choosing undulator parameters using a 1D formalism [9], the waveguide ID is optimized at 5 mm and a planar undulator with $\lambda_u = 2.7$ cm, and $B_u = 1.14$ T ($K = 2.85$) is chosen for the following simulations. Note that the fundamental mode size ($1/e$ radius of the mode amplitude) of the THz radiation inside the waveguide is around 1.5 mm. It covers the whole wiggling motion amplitude (< 700 μm) plus the electron beam transverse size (~ 220 μm).

The three-dimensional, time-dependent simulation code GENESIS 1.3 is used for modeling the FEL amplification process in the waveguide. GENESIS 1.3 solves a set of self-consistent differential equations based on Maxwell's and Hamilton's equations that describe the physics of a FEL, including the space charge effect [10].

B. Simulation results

In the simulations, we copropagate a 10 ps FWHM electron pulse and a continuous THz pulse in a simulation box with a cross section of 5 mm $\times$ 5 mm to model the conditions for a waveguide FEL amplifier. With the electron beam and undulator parameters mentioned in the previous section, we vary the peak current of electron beam and the THz seed power in order to study the amplification of the radiation pulse. The results are shown in Fig. 1. Note that electron beam energy γ is tuned to

TABLE I. Electron beam parameters for FEL simulations.

E-beam parameters	Energy	Bunch duration	Transverse size	Current	Transverse emittance
	5–14 MeV	~10 ps FWHM	~200 μm	20–80 A	5–15 mm-mrad

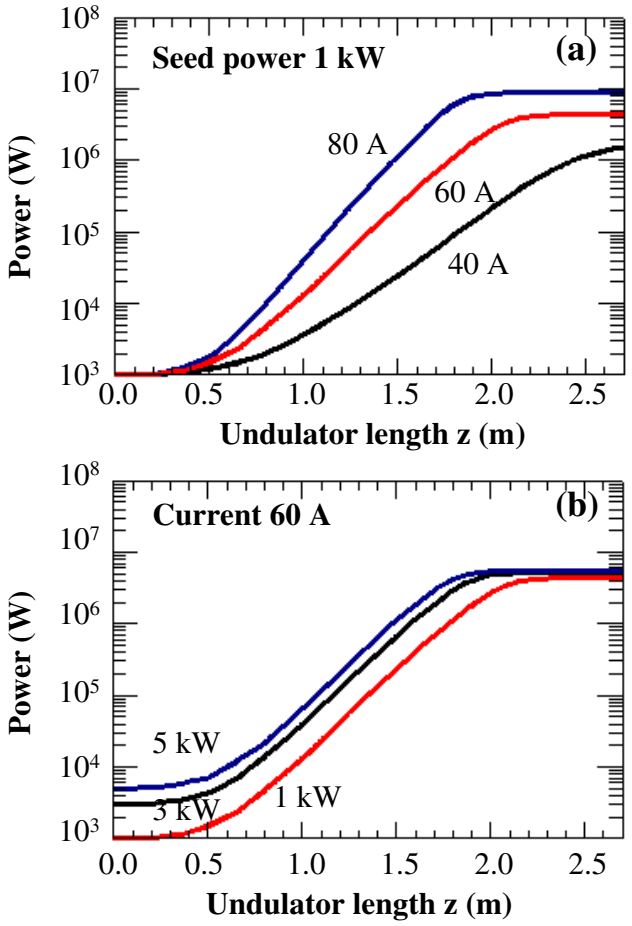

FIG. 1. (Color) Calculated THz power as a function of the undulator length z (a) for a fixed seed power of 1 kW and variable peak current of the electron beam, and (b) for a fixed peak current of 60 A and variable seed power level. Energy of the electron beam $\gamma = 19.5$, and $\lambda = 200$ μm.

fulfill the resonant condition for a waveguide FEL (e.g. $\gamma = 19.5$ for 200 μm radiation instead of $\gamma = 18.4$ in a free space) due to the phase velocity increase (longer λ_{eff}) inside the metal waveguide.

The electron beam peak current is a critical factor for the saturation power and the gain in a FEL. As shown in Fig. 1(a), for a fixed seed power of 1 kW, when the peak current increases from 40 to 80 A, the gain length (the distance for which the radiation field is amplified by a factor of e), decreases from 45 to 25 cm and the saturation power increases from 1.5 MW to ~10 MW. A higher gain for a higher peak current causes the saturation to happen over a shorter undulator length. This modeling indicates that it may be possible to reach very high peak powers on the order 100 MW for THz pulse, in a 2-m long undulator. For this, an electron pulse with a peak current of ~100 A in combination with slight tapering of the undulator for the last few periods is required.

As seen in Fig. 1(b), with a fixed beam current 60 A, a higher seed power does not significantly affect either the gain length or the saturation power level but only makes the saturation happen slightly earlier. It shows that the tolerance of the process to variations in the seed THz power is high and a ~1 kW seed pulse can be amplified to more than 4 MW in ~2 m for a relatively modest peak current of 60 A.

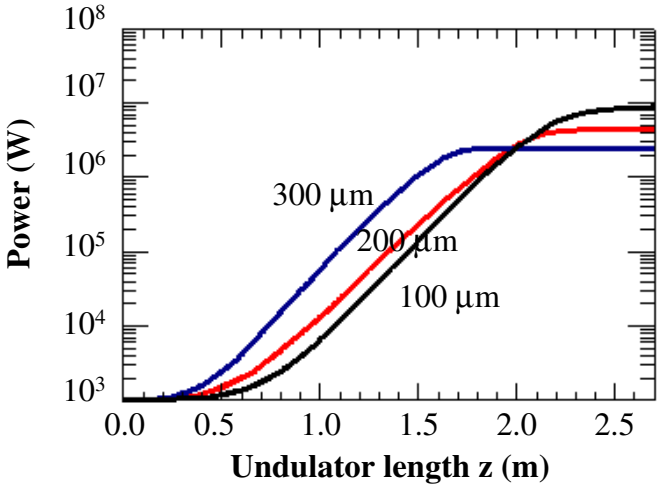

FIG. 2. (Color) Calculated THz power as a function of the undulator length z for a fixed peak current of 60 A and different wavelengths.

Spectral tunability of the optimized undulator is shown in Fig. 2. The tunability of the seeded FEL amplifier can be achieved by injecting a seed pulse with different wavelengths and an electron beam with γ matched for the resonance. Simulations were run to model three fixed wavelengths 100, 200, and 300 μm. However, full coverage of the spectral range of 0.5–3 THz is expected.

Note that, in Fig. 2, the gain and saturation power differences between various wavelengths are mainly due to the slippage effect between the electron beam and the amplified THz radiation. When the number of periods of the THz wave covering the electron bunch is smaller than the number of wiggler periods, the radiation eventually overtakes the whole electron beam and stops being amplified because of the slippage. This effect is stronger when operating at a longer wavelength and limits the overall gain of the FEL amplification.

C. FEL microbunching

Any generation of the radiation in a FEL is always accompanied by microbunching of the electron beam. The longitudinal structure of a bunched beam becomes rather complicated due to the slippage effect in a long THz FEL amplifier driven by a short electron pulse, such as that produced by a photoinjector. As seen in Fig. 3 for phase space distribution of electrons at $z = 1.4$ m, the energy modulation for different slices of the electron pulse—the width of which is equal to the seed radiation wavelength of 300 μm—is different. Because the newly

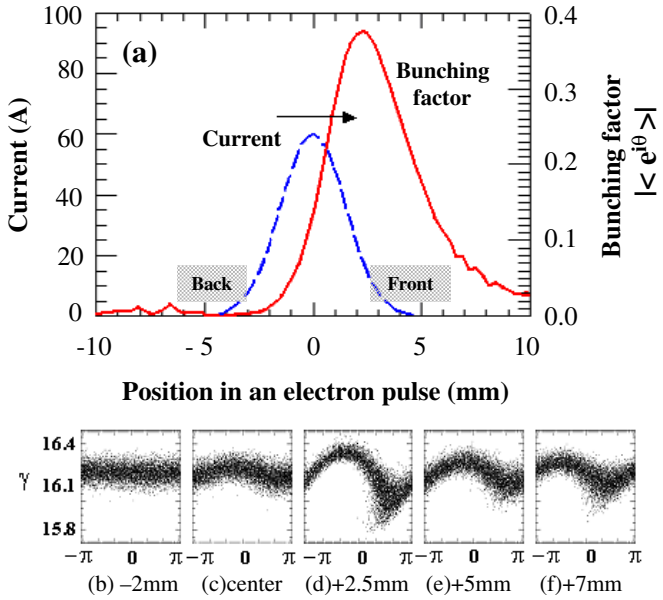

FIG. 3. (Color) Bunching factor (a) and phase space distribution at different slices (b),(c),(d),(e),(f) in the 10-ps FWHM electron pulse after the electron beam propagates 1.4 m inside undulator. The arrow shows the direction of propagation of the electron beam.

emitted radiation always overtakes the electrons that generate it, electrons constantly "see" the radiation amplified by other electrons behind them. Therefore, the energy modulation is always stronger for the electrons slightly in front of the center of the Gaussian pulse. This phenomenon results in inhomogeneous modulation of the electron beam. The bunching factor $F = |\langle e^{i\theta}\rangle|$, where θ is the phase at which each electron is located inside a period of a THz wave, is proportional to the ratio of the bunch duration and the separation between bunches. F peaks at $\sim$0.38 for electrons on the front of the electron pulse and indicates inhomogeneous microbunching [Fig. 3(a)].

Note that the energy modulation of the electron beam $\Delta\gamma/\gamma$ has a maximum of $\sim$1.25% after propagating 1.4 m inside the undulator. At this point, the phase distribution is still sinusoidal. In a longer undulator with the same 1 kW THz seed, the electron distribution folds over, which is not ideal for microbunching. Based on previous simulations using the TREDI code [11], we state that the electron beam with such magnitude of the energy modulation will be microbunched with $\sim$50% particles contained in $\sim\lambda/6$ FWHM bunches. This requires ballistic drifting of the beam over a meter or so.

It is important to study the longitudinal inhomogeneity of electron beam modulation after amplification in the FEL. It may be possible to obtain a more uniform microbunching by shaping the electron beam such that the current distribution is triangular with a slow rise time and a rapid fall rather than a Gaussian. This issue needs further study. Note that, on a THz scale, direct time-resolved measurements of longitudinal dynamics of a modulated beam are still possible using a subpicosecond streak camera.

D. IFEL/Saturated FEL microbunching

If the power of a seed pulse is far greater than the FEL saturation level, i.e., 10–100 MW for a 60 A electron beam (seen in Fig. 2), then energy is transferred from the radiation to electrons via an IFEL mechanism [12]. The IFEL in the THz range can provide more homogeneous microbunching of a relativistic electron beam in a short undulator [11,13] compared to an FEL. However, the tens of MW level of THz power needed is rather difficult but not impossible to obtain. Here we consider microbunching in a highly saturated FEL regime, where the power level of few MW is close to saturation but not above it, and strong FEL interactions take place immediately after injection of an electron beam in the undulator. This allows using a short undulator for THz bunching where the slippage effect is not yet critical.

For the undulator parameters used in the previous simulations, we study the dependence of bunching factor versus the seed power at the exit of a 30 cm long undulator. It is presented in Fig. 4. In the simulations the starting level of the seed power is 1 MW, where the deviation of THz power from the exponential region on the gain curve in Fig. 2 begins. As seen in Fig. 4, the bunching factor grows with an increase in the seed power level; however, the bunching factor F is saturated at $\sim$0.3 at approximately 50 MW of power due to the trapping of electrons in the ponderomotive well even with a short undulator.

An electron beam with a linear energy modulation can be compressed using dispersive devices, such as a chicane, to obtain a high peak current in a microbunch. As a result, an energy modulated electron beam before it is trapped is optimal for microbunching. From the simulations we conclude that, for optimal microbunching, a seed power in the range of 1–10 MW is desirable, where the electron beam

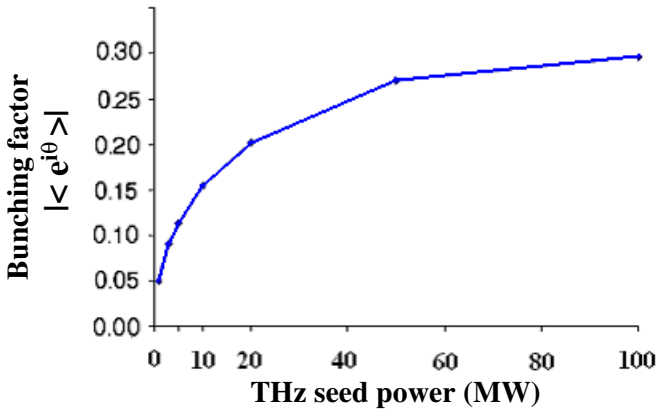

FIG. 4. (Color) Bunching factor of an electron beam after propagating in a 30 cm long, $K = 2.85$ prebuncher seeded with various powers of 100 μm pulses.

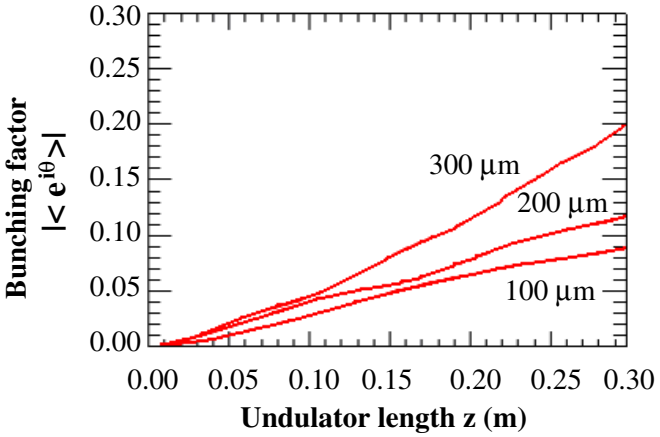

FIG. 5. (Color) Bunching factor of an electron beam copropagating with a 3 MW seed pulse with various wavelengths 100, 200, and 300 μm in a 30 cm long undulator.

modulation is linear and FEL interactions occur in a highly saturated regime. Note that this power range is experimentally achievable and it will be discussed in Sec. III A.

Microbunching in this highly saturated FEL regime for different wavelengths is shown in Fig. 5. The bunching factor of an electron beam copropagating with a 3 MW THz pulse increases along the undulator. When seeded with a longer wavelength radiation, the bunching factor increases faster due to a smaller resonant value of γ. The energy modulation of the electron beam $\Delta\gamma/\gamma$ at the exit of the undulator is $\sim$0.5%.

The bunching factor along the electron pulse in the saturated FEL regime can be seen in Fig. 6. For the same MW level of power for a seed pulse, bunching of the electron beam after the 30 cm long undulator is constant for all temporal slices as opposed to the longitudinal inhomogeneity observed for typical FEL microbunching driven by a short Gaussian electron pulse (see Fig. 3).

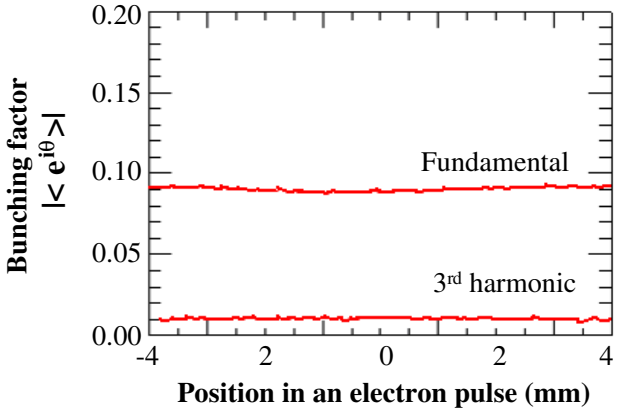

FIG. 6. (Color) Bunching factor of the fundamental and the third harmonic along a Gaussian electron pulse after 30 cm saturated FEL interaction inside the $K = 2.85$ undulator with a 3 MW seed of wavelength 100 μm.

Figure 6 also shows that the energy modulation in a planar undulator has the third harmonic components and the bunching factor of the third harmonic is approximately 1 order of magnitude less than that of the fundamental.

The fact that we observe not only microbunching at the fundamental but also for the third harmonic suggests that an undulator seeded by the prebunched electron beam can be used for HGHG process. Potential of this scheme is analyzed in Sec. IV.

In summary, simulations of the THz FEL amplifier show that by using a 10-ps long electron pulse with a modest peak current of 60 A from the typical rf photoinjector, a 1 kW seed THz pulse tunable in the range of 0.5–3 THz can be amplified to $\sim$4 MW peak power in an $\sim$2-m long undulator with $\lambda_u = 2.7$ cm, $B_u = 1.14$ T. Based on these simulations, we consider a conceptual design for a seeded THz FEL amplification at the Neptune Laboratory. It is discussed in the next section.

III. HIGH-GAIN SEEDED THZ FEL AMPLIFIER

A. Single pass THz amplifier at the Neptune Laboratory

The FEL amplifier shown in Fig. 7 consists of four subsystems: an rf photoinjector, a THz seed source, a waveguide FEL undulator, and a THz filtering system with radiation diagnostics.

The S-band photoinjector at the Neptune Laboratory can provide a 10 ps FWHM electron pulse with a peak current up to 100 A [7]. The relativistic (8–14 MeV) electron beam with an energy spread $<$0.5% and a normalized emittance $<$10 mm-mrad is propagated collinearly with a THz seed pulse through a hole in a mirror and is focused down to 220 μm (σ_{rms}) at the entrance of the undulator.

The 200 ns long THz seed pulse is generated by mixing two lines of a CO_2 laser via difference frequency generation (DFG) in a GaAs nonlinear crystal. When various pairs of CO_2 laser lines are mixed, the step-tunable THz seed radiation with a step size of 30–40 GHz is generated in the range 0.5–3 THz. This kW power THz seed radiation is focused into a waveguide within a planar, 2-m long undulator and is amplified up to 10 MW level via the FEL

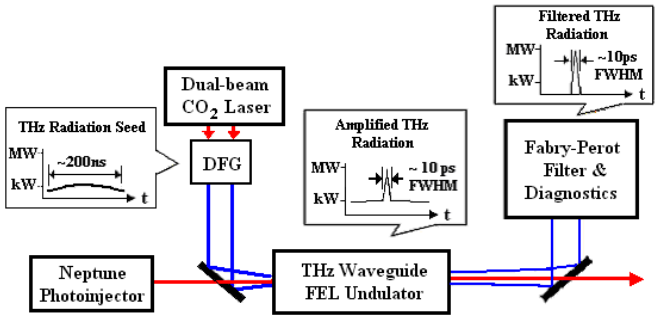

FIG. 7. (Color) Schematic of the high-gain seeded THz FEL amplifier experiment.

TABLE II. Parameters of the seeded THz FEL amplifier.

		Seeded FEL amplifier
THz Seed parameters	Wavelength	100–600 μm (0.5–3 THz)
	Seed power	~1 kW (~200 ns)
Undulator parameters	Period	2.7 cm
	K	2.85
	Length	2 m
Output THz wavelength		100–600 μm (0.5–3 THz)
Output THz power		<10 MW
Output THz pulse length		~10 ps FWHM

mechanism. Note that, even with the step-tunable CO_2 laser based seed source, the 10 ps amplified THz pulse with a transform-limited bandwidth of ~100 GHz will cover continuously the entire spectral window mentioned earlier.

After the undulator, the 200 ns long, 1 kW seed pulse is filtered by a Fabry-Perot filter. To characterize the 10 ps long, high power THz pulse, a diagnostic based on the electro-optical sampling (EOS) in combination with a fast steak camera has been considered.

In Table II, we summarize parameters and simulation results for the seed THz FEL amplifier experiment planned at the Neptune Laboratory.

B. THz source

A narrow band (< 10 GHz) THz source is necessary for seeded FEL/IFEL interactions. Recently, we developed THz radiation sources based on frequency mixing of CO_2 laser lines in a nonlinear crystal such as GaAs to provide kW and MW power pulses [5,6]. GaAs is chosen due to its high nonlinear coefficient, damage threshold, and transparency for both mid IR and THz frequencies. The THz output power at a frequency of $\omega_{\mathrm{THz}} = \omega_1 - \omega_2$ (where ω_1 and ω_2 are input CO_2 laser frequencies) can be estimated in the plane wave approximation and perfect phase matching using the following formula:

$$P_{\mathrm{THz}} = 0.5\left(\frac{\mu_0}{\varepsilon_0}\right)^{0.5}\left(\frac{4d_{\mathrm{eff}}^2\omega_{\mathrm{THz}}^2}{n_1 n_2 n_{\mathrm{THz}} c^2}\right)\frac{P_1 P_2 L^2 T_1 T_2 T_{\mathrm{THz}}}{S} e^{-\alpha L}, \tag{3}$$

where d_{eff} is the nonlinear coefficient of the crystal, S is the area of the input beams, P, n, T are power, refractive index, and the single surface transmission coefficient, respectively, with indices 1, 2, and THz corresponding to frequencies ω_1, ω_2, and ω_{THz}, α; is the absorption coefficient of the THz radiation in GaAs, and L is the interaction length.

Figure 8 shows the theoretical values of THz power calculated from Eq. (3) for a 2.5 cm long GaAs crystal and the pump power of 12 MW/cm^2 per CO_2 laser line. Three cases are calculated: DFG with no absorption for THz wavelengths (curve 1), with absorption at a room temperature GaAs (curve 2), and with absorption in a cryogenically cooled crystal (curve 3). Note that absorption data for GaAs were taken from Johnson *et al.* [14]. As shown in Fig. 8, the DFG power at a room temperature GaAs decreases below 1 kW level at 100 μm due to the strong absorption in the phonon band. However, for $T =$ 82 K, more than 1 kW is projected for the whole range of 1–3 THz.

We have built a high-repetition-rate kW power THz spectrometer tunable in the range of 0.5–3 THz for seeding FEL amplifier at kW level of power [6]. The tunability of THz generation can be achieved by mixing different pairs of CO_2 lines at the corresponding phase matching angles. Because the bandwidth of each CO_2 laser line is less than a hundred MHz, the central frequency of the newborn THz radiation is well defined and its bandwidth is transform limited by the CO_2 laser pulse length.

As for a high power THz pulse for the saturated FEL bunching described in Sec. II D, we have previously demonstrated such high power THz generation via DFG in GaAs using the Neptune TW CO_2 laser system [15]. By using 200 ps, multi-GW pump pulses in a noncollinear phase matching configuration, ~2 MW of 340 μm radiation was produced [5]. With scaling of a CO_2 laser beam spot size and larger aperture crystal, up to ~10 MW output is expected, which is sufficient for seeding an FEL buncher.

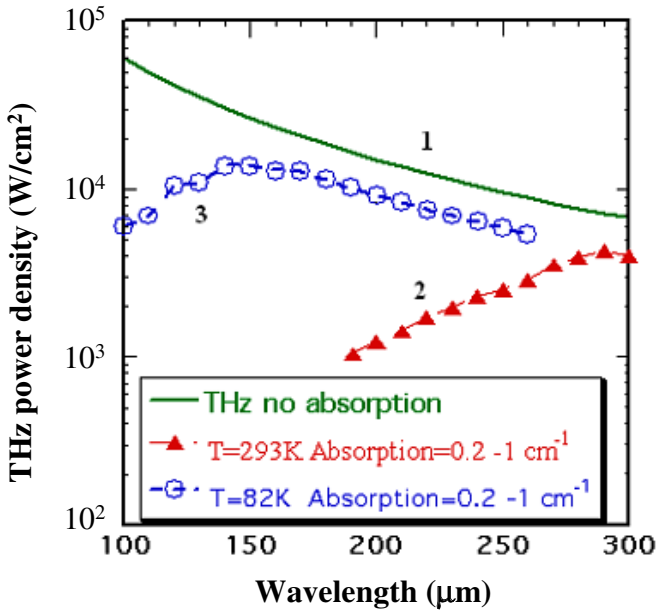

FIG. 8. (Color) THz seed generation in GaAs via difference frequency mixing (1) with no absorption for THz wavelengths, (2) with absorption at a room temperature, and (3) with absorption at a cryogenic temperature.

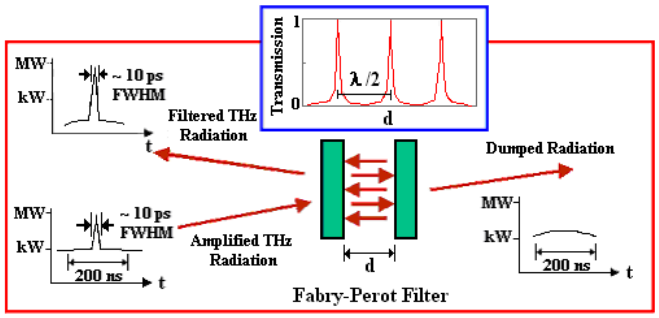

FIG. 9. (Color) Scheme for improving the THz contrast by using a Fabry-Perot filter.

C. THz filtering and radiation diagnostics

A Fabry-Perot interferometer (FPI) [16] can be used to separate a 10-ps long pulse amplified by the FEL amplifier from a 200-ns long seed pulse. Metal wire grid polarizers with a reflectivity $R > 99.9\%$ at 1 THz or GaAs plates are commercially available and can be used as reflectors to build a high finesse FPI. Therefore, it is possible to have a high transmission of the long seed pulse by finely adjusting separation between the plates d (Fig. 9 inset). However, the filling time of this Fabry-Perot cavity is on the ~10 ns scale so that the 10 ps amplified pulse will not interfere and will be directly reflected by the first surface (Fig. 9). The anticipated contrast of the 10 ps THz pulse to long 200 ns pulse can be improved up to 10^6 in a single pass.

Electro-optic sampling (EOS) is a common technique for diagnosing and characterizing a high power THz pulse [17]. The filtered 10 ps, 10 MW THz pulse can be focused onto a ZnTe crystal and combined with a linearly polarized long red pulse from a laser diode. By streaking the red pulse after the analyzer, the temporal profile of the THz pulse could be extracted.

As for the electron beam microbunching measurement, the bunched beam can be analyzed using coherent transition radiation and/or an rf cavity deflector with time resolution of 50 fs, which is under construction at the Neptune Laboratory [18]. Besides, on the THz scale direct measurement of longitudinal dynamics of electron bunches is still possible using streaking of the upconverted into visible range THz radiation.

IV. HIGH-GAIN HARMONIC THZ GENERATION

A. Proposed HGHG scheme

DFG in a GaAs crystal cannot produce seed pulses with reasonable efficiency at frequencies higher than 3 THz due to the strong phonon absorption. To extend the THz FEL output spectrum above 3 THz, we consider lasing on the third harmonic of the seed radiation using HGHG. This method has been successfully demonstrated in the visible and UV ranges [19].

In HGHG FEL, an electron beam prebunched by the fundamental radiation in the first planar undulator (prebuncher) also carries perturbations at the higher harmonics; therefore, when the prebunched beam is sent into a second undulator (radiator) designed only to resonate with the third harmonic for FEL emission, the third harmonic becomes the new fundamental in the radiator and can have a very high gain. Besides its potential to expand the frequency range of the high power THz sources, the stand alone prebuncher itself allows studying of electron microbunching at the 0.5–3 THz scale, which is important for other applications, e.g., injection of longitudinally matched beam into a plasma beatwave accelerator [4].

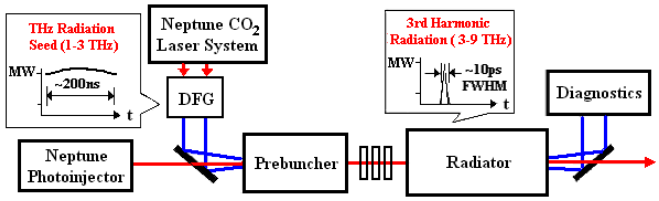

FIG. 10. (Color) Schematic of the high-gain harmonic generation arrangement.

The schematic of the HGHG experiment using the 2-m long undulator is shown in Fig. 10. We consider using a ~MW peak power THz seed pulse, generated by the Neptune TW CO_2 laser system via DFG, to modulate the electron beam energy in a 30-cm long IFEL/FEL prebuncher. After ballistic drifting, the energy-modulated electron pulse becomes a current-modulated pulse and is injected into the third harmonic radiator. A magnetic triplet is used to match the e-beam spot sizes between the two undulators.

The undulator parameters for the short prebuncher are the same as for the FEL undulator that was described in the previous section due to the identical resonant condition. As for the HGHG radiator, the K factor needs to be decreased to 1.17 from 2.85, according to Eq. (1), to fulfill the resonant condition for the third harmonic of the THz seed. This in practice can be done by increasing the gap between magnets of the long FEL undulator discussed in Secs. II and III.

B. Simulation results of THz HGHG

The GENESIS 1.3 code was used to model the whole HGHG process including the FEL prebunching, drifting/beam transverse size matching, and the FEL amplification. A 10-ps long electron beam with a peak current of 60 A is injected into the prebuncher along with a 200-ps long THz seed pulse with peak power of 3 MW. As was shown in Fig. 6, this level of seed power produces homogeneous energy modulation for the entire electron bunch in a short, 30 cm long undulator.

After drifting for a total distance of ~60 cm and passing a magnetic triplet, the electron beam has a matched spot size of 350 μm and is injected into the FEL amplifier for HGHG. Because of the energy modulation in the pre-

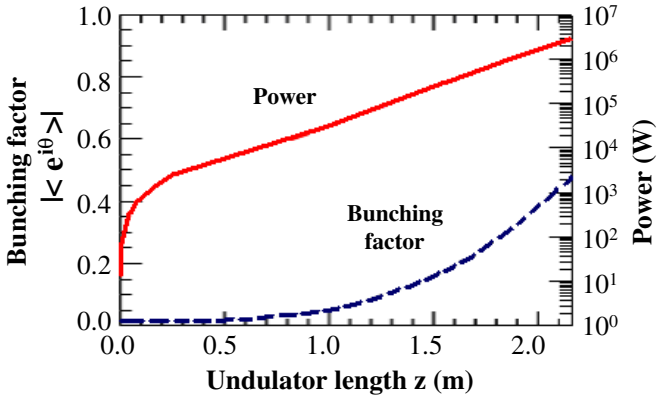

FIG. 11. (Color) Bunching factor and THz power on the third harmonic inside the HGHG radiator after injecting a prebunched electron beam with a peak current of 60 A. The electron beam is prebunched by interacting with a 3 THz pulse with a peak power of 3 MW in a 30 long prebuncher followed by ballistic drifting of 60 cm.

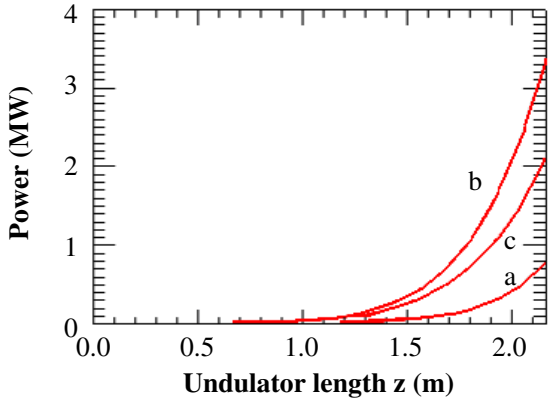

FIG. 12. (Color) Third harmonic output power vs the FEL radiator length with various power: (a) 1 MW; (b) 3 MW; (c) 10 MW of the seed pulse of wavelength 100 μm in the prebuncher.

buncher and the subsequent current bunching in the drift space, the bunching factor of the third harmonic is 4 orders of magnitude higher in comparison with that of a non-bunched electron beam. This strong current modulation shortens the length needed for building up the undulator radiation inside the FEL radiator. In Fig. 11, the bunching factor and power of the third harmonic in the radiator are presented.

By using a 3 THz pulse with a peak power 3 MW for prebunching of the electron beam, up to ~3 MW of power at 9 THz can be generated in a 216 cm long FEL radiator (solid curve in Fig. 11) resulting in the 100% conversion efficiency. As a comparison, less than 10 W can be obtained for SASE FEL with the same undulator. Slightly higher beam current can easily result in the power larger than 3 MW for a 2-m long undulator considered for the seeded THz FEL.

We also compared the third harmonic output power while varying the power of the fundamental radiation used to prebunch the electron beam (Fig. 12). Figure 12 shows that with more than 1 MW seed power and a fixed drifting distance of 60 cm, the power of the third harmonic generation is always reaching MW level in a 2 m long radiator. However, a higher seed power does not assure a higher power of the third harmonic radiation. This happens because electrons are slightly trapped instead of being sinusoidally modulated in the prebuncher when the seed radiation is too strong. Therefore, abruptly bunched electrons build up the third harmonic radiation faster at the beginning of the radiator but eventually their complicated phase space distribution hinders the gain of high harmonic generation in a longer radiator. As a result of this dynamics, there is an optimal THz seed power for prebunching electrons due to the preferable sinusoidal bunching condition at the entrance of the radiator of a given length. As is apparent in Fig. 12, for a 2 m long radiator, a 3 MW seed at 3 THz can generate ~2 MW in the third harmonic; however, using 1 MW or 10 MW seems to either underbunch or overbunch electrons in the prebuncher such that the harmonic generation in the radiator is actually reduced.

TABLE III. Parameters of the THz HGHG FEL.

		HGHG	
		Prebuncher	Radiator
Undulator parameters	Period	2.7 cm	
	K	2.85	1.17
	Length	30 cm	2 m
THz seed parameters	Wavelength	100–300 μm (1–3 THz)	
	Seed power	1–10 MW	
Output THz wavelength		33–100 μm (3–9 THz)	
Output THz power		>1 MW	
Output THz pulse length		~10 ps FWHM	

Parameters and simulation results for the HGHG FEL tunable in the range of 3–9 THz are given in Table III.

V. SUMMARY

Numerical modeling of a seeded FEL in the THz range of the electromagnetic spectrum shows that it is possible to reach high levels of >10 MW of power using a relatively short (~ 2 m long) undulator. Amplification of a seed pulse in such a device results in microbunching of the electron beam with a bunching factor of 0.3–0.4. However, due to the slippage effect this microbunching is not homogeneous for the whole electron pulse.

We have also shown that, in the highly saturated FEL regime, when amplification factor is very small, the elec-

tron microbunching is homogeneous and requires a much shorter undulator. This regime falls between the classical FEL and IFEL domains and requires a few MW level of THz seed power, when driven by an electron beam with a peak current of tens of amperes.

Based on the simulations, two FELs, driven by an electron beam from a photoinjector and seeded with a THz pulse generated via DFG using CO_2 laser lines, are considered for parameters achievable at the Neptune Laboratory at UCLA: a seeded THz FEL amplifier and a high-gain harmonic generation FEL. A 10 ps long THz pulse with a peak power up to 10 MW can be obtained in a 2-m long uniform planar undulator with a 1 kW, THz seed pulse in the waveguide FEL amplifier. In HGHG FEL configuration, $\sim$100% power conversion efficiency from the 1–3 THz seed radiation to the third harmonic can be achieved with MW level of seed power in a 30 cm long prebuncher followed by a 2-m long radiator. HGHG FEL is promising for expanding the frequency range of the high-power THz source up to 9 THz. Note that the described seed FEL scheme could be easily scalable for production of high-average power radiation in the THz range, since both high-pulse repetition CO_2 lasers and beam injectors are available.

ACKNOWLEDGMENTS

This work is supported by U.S. DOE Grant No. DE-F602-92ER40727.

[1] G. M. H. Knippels *et al.*, Phys. Rev. Lett. **83**, 1578 (1999).
[2] W. D. Kimura *et al.*, Phys. Rev. Lett. **92**, 054801 (2004).
[3] C. M. S. Sears *et al.*, Phys. Rev. Lett. **95**, 194801 (2005).
[4] S. Ya. Tochitsky *et al.*, *Advanced Acceleration Concepts*, edited by C. E. Clayton and P. Muggli, AIP Conf. Proc. 647 (AIP, New York, 2002), pp. 786–795.
[5] S. Ya. Tochitsky *et al.*, J. Appl. Phys. **98**, 026101 (2005).
[6] S. Ya. Tochitsky *et al.*, in *Proceedings of the Conference on Lasers and Electro-Optics 2006 Technical Digest* (Optical Society of America, Washington, DC, 2006), p. Ctu664.
[7] S. G. Anderson *et al.*, *Advanced Acceleration Concepts*, edited by P. L. Colestock and S. Kelly, AIP Conf. Proc. 569 (AIP, New York, 2000), p. 487.
[8] K. Halbach, in *Handbook of Accelerator Physics and Engineering*, edited by A. Chao (World Scientific, Singapore, 1998).
[9] C. Sung *et al.*, Proceedings of the 27th International Free Electron Laser Conference 2005, pp. 87–90.
[10] S. Reiche, Nucl. Instrum. Methods Phys. Res., Sect. A **429**, 243 (1999).
[11] C. Sung *et al.*, *Advanced Accelerator Concepts*, edited by V. Yakimenko, AIP Conf. Proc. 737 (AIP, New York, 2004), pp. 922–928.
[12] E. D. Courant, C. Pellegrini, and W. Zakowicz, Phys. Rev. A **32**, 2813 (1985).
[13] P. Musumeci *et al.*, *Proceedings of the International Conference on LASERS2001*, edited by V. J. Corcoran (STS Press, McLean, VA, 2002), pp. 41–48.
[14] C. J. Johnson, G. H. Sherman, and R. Weil, Appl. Opt. **8**, 1667 (1969).
[15] S. Ya. Tochitsky *et al.*, Opt. Lett. **24**, 1717 (1999).
[16] E. A. M. Baker and B. Walker, J. Phys. E **15**, 25 (1982).
[17] Q. Wu and X.-C. Zhang, Appl. Phys. Lett. **67**, 3523 (1995).
[18] R. J. England *et al.*, *Advanced Accelerator Concepts*, edited by V. Yakimenko, AIP Conf. Proc. 737 (AIP, New York, 2004), pp. 414–420.
[19] L. H. Yu *et al.*, Phys. Rev. Lett. **91**, 074801 (2003).